

Conceptual Design and Simulation Tools Applied to the Evolutionary Optimization of a Bioethanol Purification Plant

Patricia M. Hoch[†] and José Espinosa^{*‡}

PLAPIQUI-UNS-CONICET, Camino La Carrindanga km 7-8000, Bahía Blanca, Argentina, and
INGAR-CONICET-UNL, Avellaneda 3657, S3002 GJC Santa Fe, Argentina

We present an evolutionary optimization procedure applied to the design and simulation of the unit operations in a bioethanol purification plant. Conceptual and rigorous models are used; the first are utilized to determine initial values for design and operating variables, and then rigorous simulation is used to refine the results. The use of rigorous models allows for the elimination of simplifying assumptions, the interconnection of equipment, and the calculation of the operating and investment costs. Once an initial design of the purification plant is obtained, opportunities of improvement are easily recognized and then tested by performing the design and simulation steps until a cost-effective bioethanol purification plant is achieved. The methodology is applied to the purification process for a feed leaving the fermentation step of a conventional corn dry-grind processing facility producing 24 million L/year of ethanol and 19 million kg/year of distiller's dry grains with solubles (DDGS). The feed to the purification plant (22 170 kg/h) is mainly composed by ethanol (10.80% w/w) and water (88.98% w/w) with traces of methanol (0.0226% w/w) and fusel (0.2009% w/w). Following the proposed approach, two initial designs of the whole purification plant using different technologies to break the azeotrope between ethanol and water are compared in terms of operating and investment costs. Savings in overall costs of about 32% are achieved by the alternative distillation/pervaporation in comparison with the option distillation/extractive distillation. Then, the membrane-based technology is adopted as the core of the purification process and a search for further improvements is performed. Four alternative designs were evaluated. In each case, the steam consumption of the evaporation sector is reduced by 1 300 kg/h by condensing the ethanol-rich side stream from the main rectification column in the first effect of the train. Finally, the option characterized by an ethanol composition in the ethanol-rich side stream of 91.24% w/w is selected as the quasi-optimal design because overall costs are reduced by 6.67% with respect to the base case and by 11.48% with respect to the worst case analyzed.

1. Introduction

Optimization of both design and operation variables of a bioethanol purification plant intended to produce fuel-grade ethanol is a challenge to make the biofuel a realistic alternative in the energy market. While process simulation allows comparing different separation alternatives in terms of energy demand, an optimization-based approach enables the identification of the best configuration for a given superstructure, taking into account both investment and operating costs. The optimization approach is usually written in the form of a mixed-integer nonlinear programming problem, with its main drawback being that unit operations are modeled via shortcut models.¹

In this area of research, Karuppiah et al.² addressed the problem of optimizing corn-based bioethanol plants through the use of mathematical programming and heat-integration techniques. They first solved two nonlinear programming subproblems involving shortcut models for mass and energy balances for all the units in the process. Both alternatives consider the use of distillation together with molecular sieves and adsorption units with corn grits to achieve fuel-grade bioethanol. They differ from each other in the way in which the solids from the liquid in the slurry leaving the fermentor are separated. After selecting the alternative that minimizes the energy demand of the overall process, they performed a heat-integration study on it to further reduce the energy input of the plant. Despite the promising

results found, the authors suggested that simulations studies should be performed in order to validate the results presented in their contribution.

Given the plant complexity and the high nonlinearity of the corresponding models, we propose an evolutionary optimization procedure that intensively uses both conceptual and rigorous models for the design and simulation of unit operations. Finding initial values for the column design is made easier within the conceptual design environment, which is used to obtain an initial estimation of the total number of trays of the main distillation column, the placement of feed and side streams, and steam flow rate in the simulation environment. In addition, convergence of the rigorous model is enhanced by using initial estimates of internal profiles generated at the conceptual design level despite the highly nonideal behavior of the multicomponent azeotropic mixture.

Applying the same strategy to estimate initial values for other important variables, i.e., number of liquid–liquid separators and flow rate of the wash-water stream in the fusel plant, temperature and permeate pressure in the pervaporation sector (alternative distillation plus membrane sector), or ethylene glycol flow rate (alternative distillation plus extractive distillation), initial designs of bioethanol purification plants using different technologies to break the azeotrope ethanol–water are found. After selecting the best alternative in terms of overall costs, opportunities for improvement on the selected flowsheet are easily recognized and then tested by performing the design and simulation steps until a cost-effective bioethanol purification plant is achieved.

The methodology is applied to the purification process for a feed leaving the fermentation step of a conventional corn dry-

* To whom correspondence should be addressed. E-mail: destila@santafe-conicet.gov.ar.

[†] PLAPIQUI-UNS-CONICET.

[‡] INGAR-CONICET-UNL.

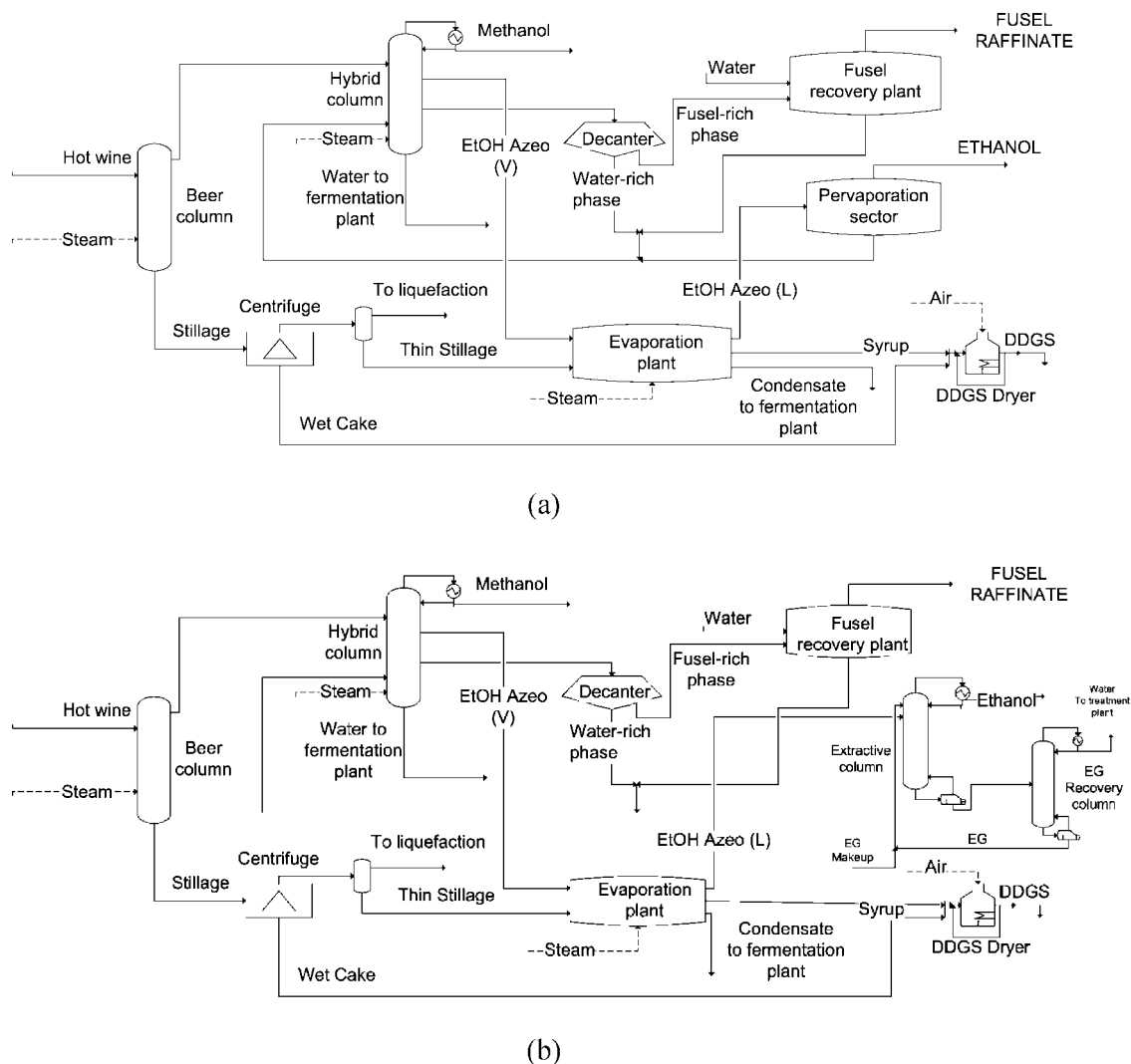


Figure 1. Simplified flow diagrams of a bioethanol purification plant: (a) alternative distillation plus pervaporation and (b) alternative distillation plus extractive distillation.

grind processing facility, producing 24 million L/year of ethanol and 19 million kg/year of distiller's dry grains with solubles (DDGS). The feed to the purification plant (22 170 kg/h) is mainly composed of ethanol (10.80% w/w) and water (88.98% w/w) with traces of methanol (0.0226% w/w) and fusel (0.2009% w/w).

2. Purification Plant Description and Design Alternatives

The bioethanol purification facility comprises a separation sector and fusel and evaporation plants. The separation sector consists of two distillation columns and either a pervaporation unit or two extra distillation columns to obtain fuel-grade ethanol.

In this work, we consider the use of either pervaporation membranes or extractive distillation with ethylene glycol to break the azeotrope between ethanol and water, but other technologies like molecular sieves^{2,3} or dehydration by selective adsorption on corn grits² may be judged as valid options.

While the first column known as "beer column" separates the solids and most of the water from a vapor stream mainly composed of ethanol and water with traces of volatile components, the main distillation column (termed hybrid distillation column) must accomplish the separation of volatile components,

which prevent the use of ethanol as fuel, and water from an ethanol–water stream with a composition near the azeotropic one.

Among the components normally present in the feed to the process,⁴ we select methanol and higher molecular weight alcohols (fusel components) because maximum concentration values for these components are set in quality standards for use of ethanol as a fuel.⁵ The feed to the purification plant (22 170 kg/h) is mainly composed of ethanol (10.80% w/w) and water (88.98% w/w) with traces of methanol (0.0226% w/w) and fusel (0.2009% w/w). Pentanol is used to approximate the thermodynamic properties of high molecular weight alcohols. Compositions were selected according to the data given by Kwiatowski et al.³ and Klosowski et al.⁴

The separation plant is integrated with two other sectors:

(i) A fusel plant with several liquid–liquid separators to avoid losses of ethanol in the fusel-rich stream leaving the hybrid column by washing the stream with water; and

(ii) An evaporation plant, where a triple-effect evaporator, a centrifuge, and a rotary dryer are used to obtain an animal feed coproduct rich in proteins (distiller's dry grains with solubles, DDGS).

Simplified flow diagrams of the two alternative processes are shown in Figure 1.

Table 1. Overall Mass Balance and Energy Demand of a Beer Column with an Infinite Number of Stages (DISTIL)

	$x_{\text{Hot wine}}$	$y_{\text{Hot wine}}^*$	x_W	s_{\min}
methanol	0.000137	0.000659	0	$(x_W - x_{\text{Hot wine}}) / (x_{\text{Hot wine}} - y_{\text{Hot wine}}^*) = 0.1753$
ethanol	0.045288	0.303358	0	
water	0.954135	0.692560	1	
1-pentanol	0.000440	0.003423	0	

Note that integration between the hybrid column and the first effect of the evaporator is performed in order to reduce the steam consumption of the latter. Once heat is exchanged between the near azeotropic vapor stream and the thin stillage from the centrifuge, the condensed ethanol-rich mixture is diverted to either the pervaporation unit or the extractive column for further dehydration.

3. Initial Design Using Pervaporation to Break the Ethanol–Water Azeotrope

3.1. Beer Column. The vapor stream leaving the stripping column captures nearly all of the ethanol and components in traces produced during the fermentation step. The minimum energy demand of the process (i.e., minimum reboil ratio) is calculated through the lever arm rule by setting the bottom product as high-purity water and the composition of the vapor stream as that corresponding to the vapor in equilibrium with hot wine. In other words, a pinch at the top of the stripping column is considered. In order to obtain a feasible design, the following steps are performed:

(1) Determine the maximum feasible separation and minimum energy demand (s_{\min}) by applying pinch theory. This task requires an equilibrium calculation that can be performed in a conceptual model framework like DISTIL.⁶

(2) Calculate the reboil ratio $s = 1.20s_{\min}$.

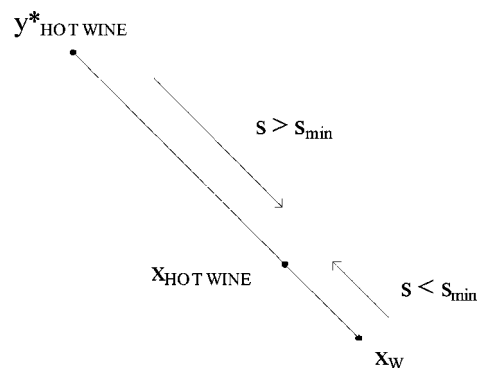
(3) Set a value for the number of stages N .

(4) Simulate a stripping column with reboiler first, and then replace the reboiler with steam, taking into account the reboiler duty and the latent heat of condensation of steam. This task can be done in a simulation framework like Hysys.⁶

Table 1 shows the “limiting” compositions of the streams entering and leaving the stripping column together with the minimum value of the reboil ratio s_{\min} . As the vapor stream leaving the stripping column is assumed to be in equilibrium with the hot wine, an infinite number of stages is required to perform the separation. Theoretically, s_{\min} represents the minimum energy demand for which pure water is obtained at the column bottom with a pinch at the column top. Reboil ratios above s_{\min} lead to a jump of the pinch region from the top to the bottom, and hence, pure water remains as the product at the column bottom. However, an increase in the water amount in the distillate is enforced, decreasing the separation power of the beer column. On the other hand, for reboil ratios below the “minimum”, the pinch is still located at column top, but alcohol is lost in the bottom product. Figure 2 schematically shows how products of a column with an infinite number of stages move along the mass balance line as the actual reboil ratio takes values above or below the minimum.

Bearing in mind the ideas above, operation of the beer column as close as possible to s_{\min} is preferred for two reasons: first, the energy demand of the process approaches its minimum value, and second, the amount of water withdrawn from the hot wine tends to its maximum value.

A quasi-optimal column design was achieved, with 38 equilibrium stages, a column diameter of 0.9 m, a section

**Figure 2.** Influence of actual reboil ratio on the products of a column with an infinite number of separation stages.**Table 2. Results for the Ternary System Ethanol/Water/1-Pentanol (DISTIL)**

	product compositions, r , s , and N
feed (vapor)	[0.29798, 0.699132, 0.002888]
distillate	[0.74144, 0.25850, 6.0 E-05]
side stream	[0.05115, 0.91442, 0.03443]
bottom	[9.6 E-06, 0.99999, 4.0 E-07]
$R_{\min}^{(1)}/S_{\min}^{(1)}$	2.839/1.00
$R^{(1)}/S^{(1)}$	2.839/1.00
$N_{\text{stages}}^{(1)}$ (including condenser and reboiler)	17 [0 + 1-15 + 16]
$N_{\text{feed}}^{(1)}/N_{\text{Side Stream}}^{(1)}$	4/11

pressure drop of 34.7 kPa, and a steam flow rate of 3600 kg/h. The values obtained for the number of equilibrium stages and steam demand, together with the composition of ethanol in the outlet stream (51.52% w/w), agree well with results presented by Kwiatkowski et al.³

3.2. Hybrid Column. As a multicomponent system formed by ethanol and water with traces of methanol and fusel is to be separated into a single column, a three-step conceptual design and rigorous simulation process is proposed.

(1) Ethanol and methanol are lumped into one pseudocomponent in order to obtain a first estimation of steam flow rate, number of stages necessary to separate an ethanol-rich stream from both a fusel-rich side stream and a water-rich bottom product, and feed stage and side stream location (DISTIL).⁶

(2) After rigorous simulation of the quaternary mixture in Hysys,⁶ separation between a methanol-rich stream and an ethanol-rich stream is considered by taking into account the distillation line departing from the composition of the distillate (DISTIL).⁶

(3) Finally, both columns are integrated into a single one (Hysys).⁶

3.2.1. Side Stream Column. In order to obtain a feasible design, the following steps are performed:

(1) Calculate $s_{\min}^{(1)}$ for the separation ethanol/water/1-pentanol (DISTIL).⁶

(2) Estimate the number of equilibrium stages $N_{\text{stages}}^{(1)}$, feed stage $N_{\text{feed}}^{(1)}$, and side stream location $N_{\text{side stream}}^{(1)}$ for $s^{(1)} > s_{\min}^{(1)}$ (DISTIL).⁶

(3) Simulate the quaternary system (Hysys)⁶ for the design and operating variables obtained in step 2.

(4) Calculate the steam flow rate $V_{\text{steam}}^{(4)}$ through the energy balance and simulate the column without reboiler (Hysys).⁶

(5) Simulate the system side stream column plus decanter and water-rich phase recycle (Hysys).⁶

Table 2 presents the results of the conceptual design performed in DISTIL,⁶ steps 1 and 2, for the ternary mixture

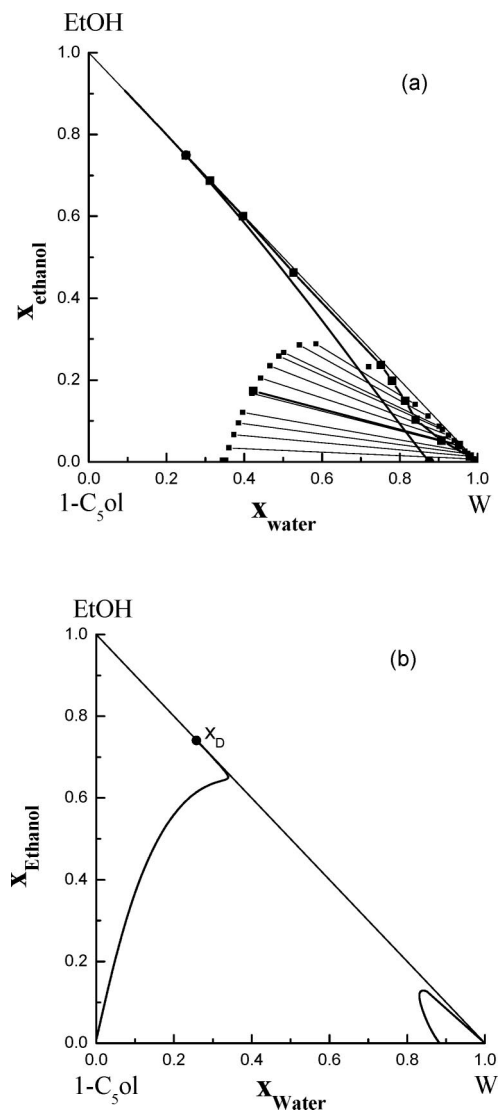


Figure 3. (a) Internal profile in the composition simplex corresponding to the base design with phase separator and water-rich phase recycle (Hysys);⁶ (b) approximate reversible profile corresponding to the distillate composition of the side stream column obtained from integration of eq 31 given by Poellmann and Blass.⁷

ethanol/water/1-pentanol, with the latter used to approximate the behavior of the component fusel. Compositions of both ethanol and fusel in the bottom stream were selected taking into account the local behavior of the residue curve corresponding to the liquid in equilibrium with the vapor feed in the neighborhood of water vertex. For both the ternary and quaternary mixtures, the corresponding residue curves approach the water vertex with compositions of ethanol above the mole fraction of fusel; therefore, the selected bottom composition reflects this behavior. Figure 3a shows the calculated composition profile in the composition simplex. The figure also shows a distillation boundary departing from the azeotrope ethanol–water and ending at the heteroazeotrope water–fusel. The side stream is located inside the liquid–liquid gap because this stream will be separated in a decanter into a fusel-rich phase (feed to the fusel plant) and a water-rich phase (recycle to column).

Note that minimum reboil ratio condition for the given separation does not require an infinite number of stages. This behavior can be understood when the reversible distillation profiles (pinch-point curves) corresponding to the selected

distillate composition are calculated. Figure 3b shows two pinch-point curves: one departing from the distillate composition and ending at pure 1-pentanol, and the other one presenting a maximum in ethanol mole fraction and joining both the heteroazeotrope and pure water. Rectifying profiles corresponding to low values of the reflux ratios end at the pinch curve located in the distillation region different from that of the distillate. On the other hand, for increased condenser energy, the rectifying profiles remain in the distillation region where the distillate is located, ending in the disjoint pinch curve near the water vertex. Between the two qualitatively different kinds of rectifying profiles, there is an adiabatic profile that bifurcates.⁷ The jump of the adiabatic profile from one pinch curve to the other, a different behavior to that encountered in ideal distillation, is responsible for the minimum energy demand without a pinch. In other words, when both the stripping and the rectifying profiles meet each other, the corresponding termination points do not belong to the internal profile of the feasible column.

3.2.2. Methanol Column and Hybrid Column. The distillate stream of the side stream column contains small amounts of methanol that must be separated from ethanol to agree with stringent quality standards (0.1% v/v methanol in dehydrated ethanol at 20 °C). At first glance, this separation could be performed in another distillation column. A different alternative would be to integrate this column with the side stream column. The distillate line (DISTIL)⁶ corresponding to the distillate composition of the side stream column shown in Figure 4a resembles the behavior of the internal profile at total reflux, and it can be considered as a good approximation to the actual operation of the methanol rectifying column, as the distillate flow rate of this column is low enough to produce a high reflux ratio. Therefore, it is possible to estimate the optimal number of stages in the rectifying section of the hybrid column as the number of trays necessary to separate the methanol in excess from the ethanol-rich stream. As shown in Figure 4a, the methanol-rich distillate stream will also contain small amounts of ethanol and water due to the distillation boundary running from pure methanol to ethanol–water azeotrope.

Figure 4b shows the internal profile in the composition tetrahedron after simulation of the hybrid column in Hysys. A loss of about 0.18% w/w of ethanol in methanol-rich distillate occurs. The side streams are located near the maximum in ethanol (ethanol-rich stream, 88.98% w/w) and fusel (fusel-rich stream, 18.5% w/w), respectively. The column has 35 equilibrium stages, a column diameter of 1.372 m, a section pressure drop of 11.8 kPa, and a steam flow rate of 1800 kg/h. The vapor ethanol-rich stream is diverted to the first effect of the evaporation sector to provide heating while minimizing the steam demand of the plant. The condensed ethanol-rich stream is then fed to the pervaporation sector to remove the excess water.

3.2.3. Fusel Plant. The fusel-rich stream leaving the decanter is fed to the fusel sector, where the stream is washed with water to recover about 96% of the incoming ethanol. The resulting water-rich stream is recycled to the hybrid column. To do this, an overall amount of 363 kg/h of wash-water and seven separation steps are necessary. The conceptual design of a cross-flow operation is performed using DISTIL,⁶ while process simulation is done in Hysys.⁶ Figure 5 shows the sequence of mass balances and equilibrium calculations obtained from Distil data.

3.2.4. Pervaporation Sector. A conceptual design of pervaporation for the polymeric composite membrane PVA/PAN

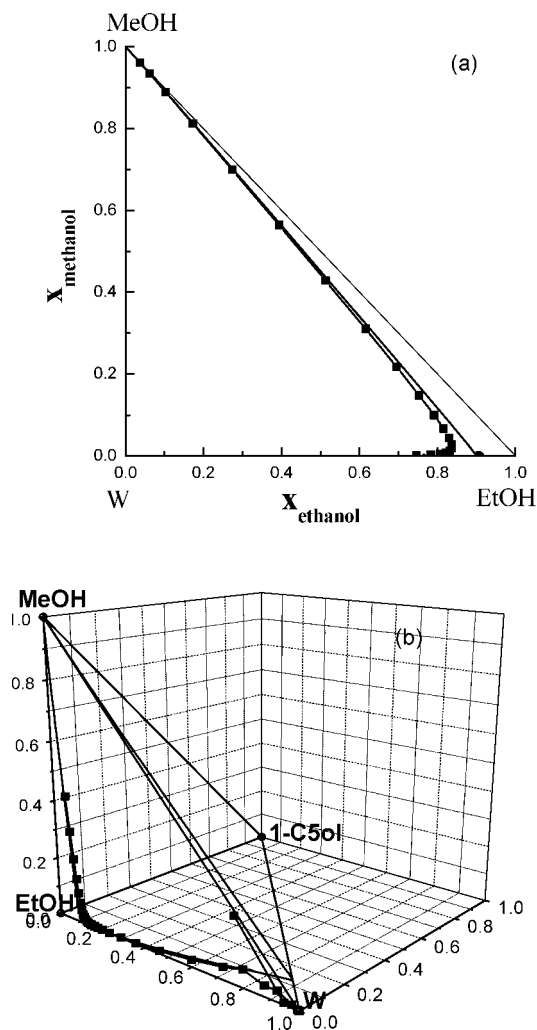


Figure 4. (a) Distillation lines corresponding to the distillate composition of the methanol column for the system methanol/ethanol/water + 1-pentanol at 101.3 kPa (DISTIL⁶). (b) Internal profile in the composition tetrahedron corresponding to the hybrid column with phase separator, fusel plant, and pervaporation sector.

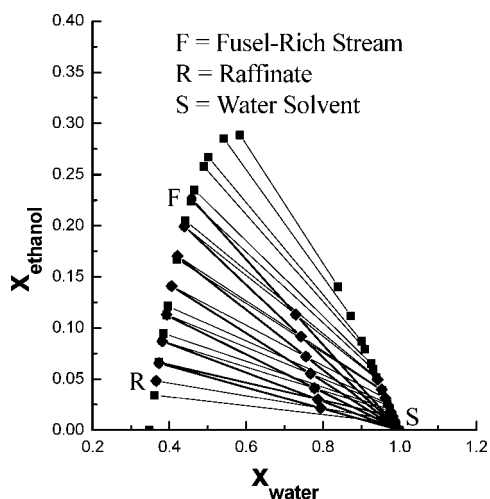


Figure 5. Estimation of number of separation steps and wash-water flow from DISTIL⁶ data at 25 °C and 101.3 kPa.

MOL 1140 (GFT, Germany) following the model proposed by Vier⁸ and Bausa and Marquardt⁹ was implemented in Delphi environment¹⁰ to determine pseudo-optimal operating values for both maximum temperature (90 °C) and permeate pressure

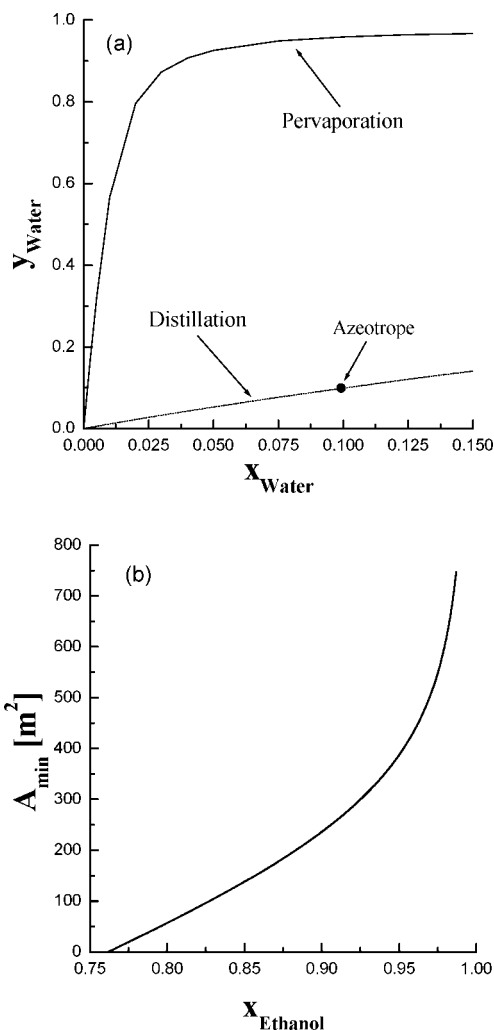


Figure 6. (a) Comparison between separation performance of pervaporation at 90 °C and 2.026 kPa and distillation at 101.3 kPa (conceptual model). (b) Minimum membrane area versus ethanol purity in the retentate (conceptual model and Hysys extension). Operation at maximum feasible temperature, 90 °C, and at a permeate pressure of 2.026 kPa.

(2.026 kPa). For these conditions, a maximum permeate flux of 1.125 kg/(m² h) is obtained.

Figure 6a shows both the permeate composition and vapor composition versus water mole fraction. It is clear that pervaporation allows for overcoming the azeotropic composition. Therefore, distillation followed by a pervaporation sector is appropriate to obtain high-purity ethanol. The hybrid process configuration with the pervaporation sector installed between two distillation columns is discarded as a separation alternative because the liquid–vapor equilibrium approaches the line $y = x$ in the region above the azeotrope, and therefore, an extremely long second column would be necessary to achieve high-purity bioethanol.

The model was also implemented in Hysys as a user operation extension,¹¹ which calculates the minimum membrane area a_{\min} by integrating the differential equations of mass balances until the desired composition of ethanol is reached at the retentate. a_{\min} is the area required considering isothermal operation. Then, the required membrane area a_{req} is calculated as $a_{\text{req}} = 1.25a_{\min}$.⁹ Bausa and Marquardt⁹ proposed the factor 1.25 by comparing different design cases with a typical temperature drop per module of 10 °C with their corresponding minimum membrane area. Removing the assumption of isothermal operation and using the energy balance to model the temperature drop in each

Table 3. Operation (\$/ton DDGS) and Investment (\$) Cost Corresponding to DDGS Plant

item	characteristics	(invest./op. costs) ¹³	(invest./op. costs) ^b ¹⁵
rotary dryer	D (m) = 1.664 L (m) = 13.31 τ (min) = 19.6 rpm = 2.869 Q_{air} (kg/h) = 39 150 $\eta_{\text{nat. gas}}$ = 0.048 ^a	(1.39 E+06)/19.74	1.57 E+06
evaporator	area _{overall} (m ²) = 940 pressure (kPa) = from 10 to 30 kPa Q_{steam} (kg/h) = 2 700	(1.523 E+06)/16.16	1.47 E+06
decanter centrifuge		(1.07 E+06) ^c /1.357	1.07 E+06

^a (kg of natural gas)/(kg of water evaporated). ^b Overall operating costs = 34.55 \$/ton of DDGS. ^c Calculated from Battelle M. I.¹⁵

module (and also reheating between modules as shown by Daviou et al.¹¹) led to similar results. Both heat and refrigeration duties are calculated in Hysys from the energy balances. Behavior of trace components is taken into account by using water–alcohol separation factors. Approximate values were taken from Van Baelen et al.¹² Figure 6b shows the minimum membrane area versus ethanol mole fraction in the retentate leaving the pervaporation sector. High-purity bioethanol (99.5% v/v) is obtained with an actual membrane area of 930 m², while the water-rich permeate is recycled to the hybrid column.

3.2.5. DDGS Plant. The coproduct plant is formed by a decanter centrifuge that separates the bottom stillage from the beer column in a wet cake (35% solids, 2 683 (kg of water)/h) and a thin stillage (18 443 (kg of water)/h). Approximately 4 626 (kg of water)/h is recycled into the second step of the liquefaction process, while 13 817 (kg of water)/h is fed to a three-effect evaporator. The resulting syrup (35% solids, 1 287 (kg of water)/h) is mixed with the wet cake coming from the centrifuge and sent to a rotary drum dryer. While the multiple-effect evaporator is simulated in Hysys,⁶ only mass and energy balances for the dryer are incorporated in Hysys.⁶ The conceptual design of the dryer is performed according to the method presented by Ulrich and Vasudevan¹³ and data from National Corn-To-Ethanol Research Center.¹⁴ Table 3 summarizes the investment and operation costs of the DDGS sector. The operation cost of 37.3 \$/ton of DDGS agrees well with the value reported by Batelle Memorial Institute.¹⁵ A detailed cost model is shown in Appendix A.

4. Initial Design Using Ethylene Glycol to Break the Ethanol–Water Azeotrope

Another process alternative to obtain high-purity bioethanol is the use of a high boiling solvent to break the azeotrope formed by ethanol and water. In this case, the pervaporation sector is replaced by two distillation columns. The ethanol-rich stream, with a composition slightly below the azeotrope, is fed to the extractive column. There, ethylene glycol is added near the column top to extract the water, while pure ethanol is recovered at column top. The bottom product, a mixture formed mainly by ethylene glycol and water, is diverted to the second column, where water is removed at the top and the solvent is recovered at the bottom, in order to recycle it to the extractive column.

Figure 7 shows both the internal profile and the overall mass balance corresponding to the extractive column. Three separation regions can be identified from bottom to top: separation of ethylene glycol (EG) from a mixture of EG and water, separation of ethanol from a mixture ethanol/water/EG with composition

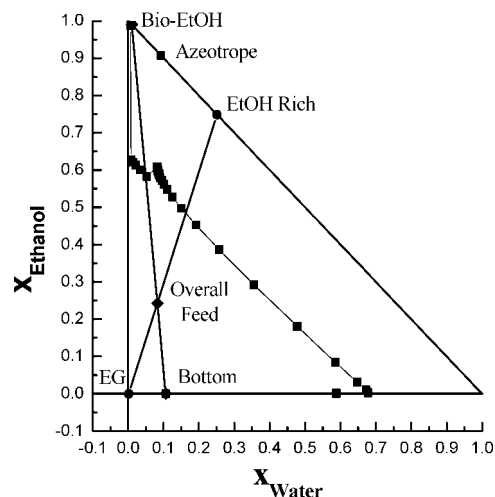


Figure 7. Internal profile and mass balance lines corresponding to the extractive distillation column. System methanol + ethanol, water + 1-pentanol, and ethylene glycol at 101.3 kPa.

Table 4. Investment and Operating Costs Corresponding to the Separation Plant; Alternative Distillation Plus Extractive Distillation

item	investment, \$	operating, \$/h	investment, \$/h	total, \$/h
beer column	3.011 E+05	52.66	6.12	58.78
hybrid column	5.065 E+05	26.33	10.30	36.63
extractive column	9.141 E+05	118.90	18.59	137.49
EG recovery col.	8.472 E+04	12.53	1.72	14.25
others	5.845 E+05	13.98	11.89	25.87
whole plant	2.391 E+06	224.4	48.63	273.03

Table 5. Mass (kg/h) and Energy (kJ/h) Streams Corresponding to a Feasible Design for the Separation Plant Formed by Two Distillation Columns, The Fusel Plant and the Pervaporation Sector

component	mass and energy flowrates, column design parameters		
	hot wine	steam beer column	stillage
MeOH	5.0214		4.5344 E–03
EtOH	2394.4		3.0620 E–07
water	19726	3603	21126
1-C5ol	44.532		3.0768 E–18
stream name	steam hybrid column	bottom hybrid column	methanol
MeOH		36.0091 E–05	2.4389
EtOH		6.2238 E–04	4.2863
water	1801.51	4350.3	0.17666
1-C5ol		2.5493 E–06	2.2251 E–20
stream name	ethanol	fusel raffinate	
MeOH	2.5776	3.1159 E–05	
EtOH	2389.5	0.55056	
water	12.275	5.0612	
1-C5ol	0.39053	44.142	
stream name or equipment	condenser duty hybrid column	beer column	hybrid column
	8.41 E+06	38 stages ΔP (kPa) = 34.7 diameter (m) = 0.914	35 stages+condenser ΔP (kPa) = 16.7 diameter (m) = 1.372

of EG almost constant, and purification of ethanol from a mixture ethanol/EG. The second column (not shown) is operated at 40.8 kPa to reduce the boiling point of EG according to the suggestion given by Sommer and Melin.¹⁶ In line with the results obtained for the mentioned authors for the system 2-propanol/water, the hybrid process distillation/pervaporation is more profitable than the system distillation/extractive distillation. Investment and operating costs for this alternative are shown in Table 4. Taking into account both operating and investment costs (see Table 6 below), savings of about 32% is achieved with the hybrid process; therefore, it is adopted for making further improvements.

Table 6. Investment and Operating Costs Corresponding to the Separation Plant; Alternative Distillation Plus Pervaporation

item	investment, \$	operating, \$/h	investment, \$/h	total, \$/h
beer column	3.011 E+05	52.66	6.12	58.78
hybrid column	5.932 E+05	39.73	12.06	51.79
membrane sector	2.837 E+06	27.14	57.70	84.84
others	1.881 E+05	5.67	3.82	9.49
whole plant	3.9194 E+06	125.2	79.70	204.90

5. Evolutionary Optimization

Table 5 presents the overall mass and energy streams of the separation plant corresponding to the base case analyzed. Steam at a pressure of 405.2 kPa and at a temperature of 150 °C is fed at the bottom of both columns. Number of stages, diameter, and pressure drop are also given. Table 6 shows the related investment and operating costs.

A cost of 400.0 \$/h or 0.1325 \$/L is the contribution of both the separation and the coproduct processing plants to the overall ethanol production cost. This value agrees well with the cost reported by Kwiatowski et al.³

Once an initial design was obtained, the following improvement opportunities were tested: (i) design of the beer column in the neighborhood of minimum energy demand (done from the very beginning of design process), (ii) heat integration between the hybrid column and the evaporation first effect (1270 kg/h of steam are saved), and (iii) heat recovery from the hot air leaving the dryer (saving 0.014 (kg of natural gas)/(kg of water evaporated)).

Note that integration between the hybrid column and the first effect of the evaporator is performed in order to reduce the steam consumption of the latter and to condense the stream that has to be liquid for feeding the pervaporation membrane module. Once heat is exchanged between the near azeotropic vapor stream and the thin stillage from the centrifuge, the condensed ethanol-rich mixture is diverted to the pervaporation plant for further water reduction. A 31% reduction in the steam demand of the evaporation sector is achieved. The result obtained encourages a further study of integration possibilities. However, a proper heat integration analysis should include the fermentation plant to take into account hot and cold streams across the whole plant.

Finally, a change in distillate composition of the hybrid column is proposed in order to capture the trade-offs between distillation and pervaporation costs. Resorting again to the

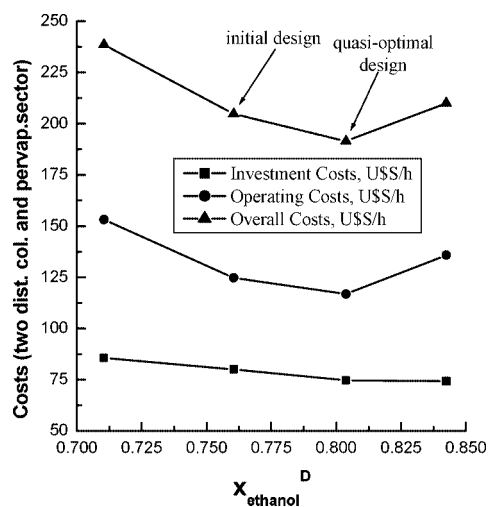


Figure 8. Overall investment and operating costs for the two distillation columns and pervaporation sector versus ethanol mole fraction in the distillate of the hybrid column.

Table 7. Overall Costs for a Bioethanol Purification Plant Producing 24 Million L/Year; The Facility Considers Both the Ethanol and Coproduct Processing Plants

	investment, \$	operating \$/h	investment, \$/h	total, \$/h
DDGS plant	3.985 E+06	96.37	81.07	177.44
separation	3.768 E+06	117.96	76.66	194.62
total	7.753 E+06	214.33	157.73	372.06

conceptual design of the hybrid column for a set of distillate compositions, results shown in Figure 8 are obtained. The decrease of investment costs for distillate compositions richer in ethanol is related to a decrease in the membrane area needed to obtain dehydrated bioethanol ($a_{\text{req}} = 848 \text{ m}^2$). The minimum in the operation costs corresponds to a minimum in the steam flow rate of the hybrid column (1 600 kg/h). The water processed in the pervaporation sector decreases from 13.5% w/w (base case) to 10.4% w/w (quasi-optimum operation). The weight percent in both cases are calculated from the water flow rate entering the hybrid column. Table 7 shows both investment and operating costs of the quasi-optimal purification plant. All cases include improvements (i), (ii), and (iii) mentioned above. Investment and operation costs are reduced by 6.67% with respect to the base case and by 11.48% with respect to the worst case analyzed.

6. Conclusions

A cost-effective design for a bioethanol separation plant using conceptual design followed by rigorous simulation is found. The advantage of the method is that the systematic use of conceptual models allows the designer to capture the main characteristics of each operation involved in the process.

In line with this statement, the minimum in the operation costs shown in Figure 8 corresponds to a minimum in the steam flow rate of the hybrid column (1600 kg/h). This minimum in steam flow rate can be only explained by the presence of the fusel component, which influences both the energy demand and the feasible products of the hybrid column. Therefore, designs based on the binary system ethanol–water do not represent the system behavior in an accurate way. From this consideration emerges the importance of properly determining the amount of trace components that enter the purification process. From the analysis of the results obtained, it is also clear that the investment cost corresponding to the membrane sector is high enough to promote future research efforts in testing both selectivity and flux behavior of other commercial pervaporation membranes.

Acknowledgment

This work was supported by UNL & ANPCyT (PICTO No. 36020), UNS PGI (24/M104), and CONICET (PIP No. 5914) from Argentina.

Appendix A: Cost Model

Investment costs are annualized using the following expression:

$$a = \frac{i(i+1)^y}{(i+1)^y - 1} (1/\text{year}) \quad (\text{A.1})$$

where a is the annuity, i is the interest rate, and y is the lifetime (years).

For the case of membrane replacement, $y = 3$; for the rest of the equipment, $y = 10$. The plant operates 8000 h/y. Costs are updated using the factor (CEPCI/400), where CEPCI is the updated Chemical Engineering Plant Cost Index.

A.1. Pervaporation Sector

A.1.1. Investment Cost. Purchase cost of the membrane equipment is referenced to the total area a_{req} . Optimization is performed considering a_{req} despite the fact that membrane modules can be purchased by units of fixed area. Once the optimal area is obtained, the final cost will be found by rounding to the highest integer the ratio a_{req}/a_{mod} to find the number of modules.

$$C_{P,M} = \alpha_{memb} a_{req} \quad (A.2)$$

$$C_{PV}^{inv} = 7.63 C_{P,M} \quad (A.3)$$

where

$$\alpha_{memb} = 400 \text{ \$/m}^2$$

A.1.2. Operating Cost. Operating cost of the pervaporation sector (C_{PV}^{op}) includes refrigeration to condense the permeate and keep vacuum (C_{refrig}), reheating between stages to keep the temperature level (C_{heat}), and the replacement cost of membranes (C_{repl}).

$$C_{PV}^{op} = C_{refrig} + C_{heat} + C_{repl} \quad (A.4)$$

where

$$C_{refrig} = \alpha_{refrig} Q_{refrig} \quad (A.5)$$

$$C_{heat} = \alpha_{vapor} \sum_{i=1}^m Q_{stages} \quad (A.6)$$

$$C_{repl} = \alpha \alpha_{memb} a_{req} / 8000 \quad (A.7)$$

where α_{refrig} and α_{vapor} are the costs of refrigerant and steam (\$/kWh), α_{memb} is the membrane cost (\$/m²), and Q_{refrig} and Q_{stages} are the heat requirements (kW) in the condenser of the permeate stream and between modules, respectively. The following values were used:

$$\alpha_{refrig} = 3.824 \times 10^{-2} \text{ \$/kWh}$$

$$\alpha_{vapor} = 2.396 \times 10^{-2} \text{ \$/kWh}$$

$$\alpha_{memb} = 400 \text{ \$/m}^2$$

A.2. Distillation Sector

Cost expressions are obtained from data from Ulrich and Vasudevan¹³ unless noted otherwise.

A.2.1. Investment Cost.

Shell.

$$C_{shell} = C_{C,shell} F_{BM} f_q \quad (A.8)$$

with

$$\begin{aligned} C_{C,shell} &= 1780 L^{0.87} D^{1.23} \\ F_{BM} &= 1.7133 F_P F_M + 2.5867 \\ F_P &= 1 \quad P < 5 \text{ barg} \\ F_M &= 2.4 \\ f_q &= 1.534 \end{aligned} \quad (A.9)$$

where $C_{C,shell}$ is the purchase cost of shell (\$), P is the operating pressure (barg), L height (m), D is the diameter (m), F_M is the material factor, F_{BM} is the bare module factor, and f_q is the contingency and fee factor.

Stages.

$$C_{stages} = C_{C,stage} F_{BM,stage} N_p f_q / f_{NST} \quad (A.10)$$

with

$$\begin{aligned} C_{C,stage} &= 464.16 D_{col}^{2.2146} \\ F_{BM,stage} &= 2.2 \\ f_q &= 1.534 \end{aligned} \quad (A.11)$$

where $C_{C,stage}$ is the cost of purchase of one stage (\$); N_p is the number of distillation stages; f_{NST} is the correction factor for low number of stages, in this case $f_{NST} = 1$ for $N_p > 20$; $F_{BM,stage}$ is the bare module factor; and f_q is the contingency and fee factor.

Heat Exchangers.

$$C_{BM,HE} = f_q C_{C,HE} (1.3077 F_P F_M + 1.6923) \quad (A.12)$$

where $C_{C,HE}$ is the purchase cost of heat exchanger (\$), which is different for condenser and reboiler. Because both distillation columns have no reboilers because live steam is fed at the bottom of the column, the reboiler cost expression is not shown. Also, P is the operating pressure (barg) and F_M is the material factor.

For the pressure, material, and contingency and fee factors, the following values were used:

$$\begin{aligned} F_P &= 1 \\ F_M &= 2.4 (\text{SS304}) \\ f_q &= 1.534 \end{aligned} \quad (A.13)$$

Floating-Head Heat Exchangers (Condenser).

$$C_{C,HE} = 450 A_{HE}^{0.7} \quad (A.14)$$

Centrifugal Pumps.

$$C_{pump} = C_{C,pump} F_{BM,pump} f_q \quad (A.15)$$

$$C_{C,pump} = 1912.5 \omega_s + 1401.7 \quad (A.16)$$

$$\omega_s = \frac{q \Delta P}{\varepsilon_i} \quad (A.17)$$

where $C_{C,pump}$ is the purchase cost (\$), q is the volumetric flow (m³/seg), ε_i is the efficiency ($\varepsilon_i = 0.8$), ω_s is the shaft power (kW), $F_{BM,pump}$ is the bare module factor for pumps, calculated as follows:

$$F_{BM,pump} = 1.5 F_{P,pump} F_{M,pump} + 2.0148 \quad (A.18)$$

For working at low discharge pressures, a correction factor is used ($F_{P,pump}$)

$$F_{P,pump} = 0.7823 \ln(p_i) - 0.8451 \quad p_i > 10 \text{ barg} \quad (A.19)$$

$$F_{P,pump} = 1 \quad p_i < 10 \text{ barg} \quad (A.20)$$

As before, f_q is used as a contingency and fee factor, $f_q = 1.534$.

Distillation Column.

$$C_{DST}^i = \sum C_k \quad \text{with } k = \text{shell, stages, HE, pump} \quad (A.21)$$

Generic Heat Exchangers.

$$C_{C,HE} = 1144.16 A_{HE}^{0.65} \quad (A.22)$$

$$C_{BM,HE} = C_{C,int} F_{BM,int} \quad (A.23)$$

$$C_{HE} = f_q C_{BM,HE} \quad (A.24)$$

$$F_{BM,HE} = (1.3077 F_P F_M + 1.6923) \quad (A.25)$$

$$f_q = 1.534$$

A.2.2. Operating Cost.

$$C_{DST}^{op} = C_{cond} + C_{reb} \quad (A.26)$$

$$C_{cond} = \alpha_{CW} \frac{Q_{cond}}{\Delta T_{CW}} \quad (A.27)$$

$$C_{reb} = C_{steam} Q_{reb} \quad (A.28)$$

$$C_{pump} = C_{electricity} \omega_s \quad (A.29)$$

$$\alpha_{CW} / \Delta T_{CW} = 5.73 \times 10^{-3} \text{ (\$/kW)}$$

$$\alpha_{steam} = 2.396 \times 10^{-2} \text{ (\$/kW)}$$

$$\alpha_{electricity} = 0.08 \text{ (\$/kW)}$$

Q_{cond} is the condenser duty (kW), Q_{reb} is the reboiler duty (kW), $\Delta H_{vap} = 39\,560$ kJ/kmol is used to relate reboiler duty with live steam heat duty, which for simplicity is referred to as Q_{reb} .

A.2.3. Overall Cost.

$$C_{DST,i} = C_{DST,i}^{inv} + C_{DST,i}^{op} \quad (A.30)$$

A.3. Fusel Plant

Eight vessels and a heat exchanger are found in the fusel plant. The costs can be calculated using the expressions already shown for the parts of a distillation column.

A.4. Evaporation and Drying

There are three single-effect evaporators, three pumps, and a condenser, plus the drying unit having a rotary dryer and a centrifuge.

Evaporators.

Evaporators are dimensioned according to the heat exchanged. The global heat exchange coefficient depends on the concentration °Brix_i of the stream processed by effect *i*, and it is related to the flowrate according to the following expressions (Radovic et al.,¹⁷):

$$U_{evap,i} = 1674.4 \text{ }^\circ\text{Brix}_i/T_i \quad (A.31)$$

where

$$\text{ }^\circ\text{Brix}_i = 1765/(1765 + M_i) \times 100 \quad (A.32)$$

M_i is the flowrate of the stream in effect *i* and T is the temperature of effect *i*. UA is provided by the simulation, and thus, the area for each effect can be calculated. The cost for each effect is calculated as the cost for a falling-film evaporator.

$$C_{c,evap,i} = 666.5515A_i^{1.0070} \quad (A.33)$$

$$C_{BM,i} = f_q C_{c,evap,i} F_{BM} \quad (A.34)$$

As before, the contingency and fee factor used is $f_q = 1.534$. Pumps and condenser costs are found using the expressions already shown in the hybrid distillation-pervaporation sector.

Centrifuge.

Investment cost for the centrifuge is taken from the report of the Battelle Memorial Institute.¹⁵ The power required to operate the centrifuge depends on the diameter,

$$\text{BHP}_{\text{centrif}} = 74.1 D_{\text{centrif}}^{2.1} \quad (A.35)$$

where the diameter

$$D_{\text{centrif}} = 0.0165(\text{dry DDGS} [\text{lb/h}])^{0.462} \text{ (ft)} \quad (A.36)$$

Dryer.

The cost for a rotary dryer is as follows:

$$C_{\text{BM,dryer}} = f_q C_{\text{P,dryer}} F_{\text{BM}} \quad (A.37)$$

$$C_{\text{P,dryer}} = 28202.99 V_{\text{dryer}}^{0.378} \quad (A.38)$$

$$F_{\text{BM}} \text{ for SS304} = 4.5$$

$$f_q = 1.534$$

The cost calculated using this expression includes the cost of the impeller. The power required to rotate the dryer is found with the following dimensional equation:

$$\text{BHP} = \frac{N \times (4.75d \cdot w + 0.1925D \cdot W + 0.33W)}{100000} \quad (A.39)$$

where BHP is the brake horsepower (kW), N is the rotating speed (rpm), d is the shell diameter (ft), D is $d + 2$ (ft), W is the complete weight of equipment plus material to be dried (lb), and w is the weight of material to be dried (lb).

The dryer works because there is a stream of warm air entering and evaporating a fraction of the water contained in the cake. Air enters at a temperature of 315 °C and goes out at 100 °C. These values are in good agreement with the literature. Heat to be provided is calculated assuming that 90% of the water in the cake has to be eliminated. This value (Q_{sec}) is calculated from a mass balance (Hysys). Specific enthalpies are calculated, so the mass of air required M_{air} can be found as follows:

$$M_{\text{air}} = Q_{\text{sec}} / (H_{\text{out}} - H_{\text{in}}) \quad (A.40)$$

Air is heated with a natural gas heater. The cost of natural gas is taken as 0.289 (\$/kg).

Literature Cited

- (1) Mussati, M. C.; Aguirre, P. A.; Espinosa, J.; Iribarren, O. A. Optimal Design of Azeotropic Batch Distillation. *AIChE J.* **2006**, *52* (3), 968–985.
- (2) Karupiah, R.; Peschel, A.; Grossmann, I. E.; Martín, M.; Martinson, W.; Zullo, L. Energy Optimization for the Design of Corn-Based Ethanol Plants. *AIChE J.* **2008**, *54* (6), 1499–1525.
- (3) Kwiatkowski, J. R.; McAloon, A. J.; Taylor, F.; Johnston, D. B. Modeling the Process and Costs of Fuel Ethanol Production by the Corn Dry-Grind Process. *Ind. Crops Prod.* **2006**, *23*, 288–296.
- (4) Klosowski, G.; Czuprynski, B.; Wolska, M. Characteristics of alcoholic fermentation with the application of *Saccharomyces cerevisiae* yeasts: As-4 strain and I-7-43 fusant with amyolytic properties. *J. Food Eng.* **2006**, *76*, 500–505.
- (5) IFQC. Setting quality standard for fuel ethanol; DEH Ethanol Standard 18/2004 Report; International Fuel Quality Center, Hartdownstream Energy Services: Houston, TX, 2004.
- (6) Hysys & Distil User Manuals; Hyprotech Ltd.: Calgary, Canada, 1999.
- (7) Poellmann, P.; Blass, E. Best Products of Homogeneous Azeotropic Distillation. *Gas Sep. Purif.* **1994**, *8* (4), 194–228.
- (8) Vier, J. *Pervaporation azeotroper wässriger und rein organischer Stoffgemische-Verfahrensentwicklung und -integration*. Ph.D. Thesis, Institut für Verfahrenstechnik, RWTH Aachen, Shaker Verlag, Aachen, Germany, 1995.
- (9) Bausa, J.; Marquardt, W. Shortcut Design Methods for Hybrid Membrane/Distillation Processes for the Separation of Nonideal Multicomponent Mixtures. *Ind. Eng. Chem. Res.* **2000**, *39*, 1658–1672.
- (10) Borland Delphi 3; Copyright 1997 Borland International, Inc., Scotts Valley, CA.
- (11) Daviou, M. C.; Hoch, P. M.; Eliceche, A. M. Design of Membrane Modules Used in Hybrid Distillation/Pervaporation Systems. *Ind. Eng. Chem. Res.* **2004**, *43*, 3403–3412.
- (12) Van Baelen, D.; Van der Bruggen, B.; Van den Dungen, K.; Degreve, J.; Vandecasteele, C. Pervaporation of water–alcohol mixtures and acetic acid–water mixtures. *Chem. Eng. Sci.* **2005**, *60*, 1583–1590.
- (13) Ulrich, G. D.; Vasudevan, P. T. *Chemical Engineering Process Design and Economics: A practical guide*, 2nd ed.; Process Publishing: Durham, NH, 2004.
- (14) National Corn-To-Ethanol Research Center. Utilizing the National Corn-to-Ethanol Pilot Plant to Develop a Predictive Model for Distillers Dried Grain for the Fuel Ethanol and Animal Feed Industries, 2005–2007.
- (15) Quantifying Biomass Resources for Hydrothermal Processing II; Battelle Memorial Institute, Pacific Northwest Division: Richland, WA, 2005.
- (16) Sommer, S.; Melin, T. Design and Optimization of Hybrid Separation Processes for the Dehydration of 2-Propanol and Other Organics. *Ind. Eng. Chem. Res.* **2004**, *43*, 5248–5259.
- (17) Radovic, L. R.; Tasic, A. Z.; Grozdanic, D. K.; Djordjevic, B. D.; Valent, V. J. Computer Design and Analysis of Operation of a Multiple-Effect Evaporator System in the Sugar Industry. *Ind. Eng. Chem. Process Des. Dev.* **1979**, *18* (2), 318–323.

Received for review March 25, 2008

Revised manuscript received July 14, 2008

Accepted July 23, 2008

IE800450A